

General Disclaimer

One or more of the Following Statements may affect this Document

- This document has been reproduced from the best copy furnished by the organizational source. It is being released in the interest of making available as much information as possible.
- This document may contain data, which exceeds the sheet parameters. It was furnished in this condition by the organizational source and is the best copy available.
- This document may contain tone-on-tone or color graphs, charts and/or pictures, which have been reproduced in black and white.
- This document is paginated as submitted by the original source.
- Portions of this document are not fully legible due to the historical nature of some of the material. However, it is the best reproduction available from the original submission.

NSG 1324

Interaction Between a Normal Shock Wave
and a Turbulent Boundary Layer
at High Transonic Speeds
Part II. Wall Shear Stress

by

M. S. Liou* and T. C. Adamson, Jr.

Department of Aerospace Engineering
The University of Michigan
Ann Arbor, Michigan 48109, U.S.A.

(NASA-CR-158542) INTERACTION BETWEEN A
NORMAL SHOCK WAVE AND A TURBULENT BOUNDARY
LAYER AT HIGH TRANSONIC SPEEDS. PART 2:
WALL SHEAR STRESS (Michigan Univ.) 41 p HC
A03/MF A01

N79-23010

Unclas
20859
CSCL 01A G3/02



* Present address: Flight Sciences Dept., McDonnell Douglas Research Laboratories, Box 516, St. Louis, Missouri 63166, U.S.A.

1. Introduction

When a shock wave impinges upon a wall, it penetrates the boundary layer along the surface and both the shock wave and the boundary layer are changed from their undisturbed states. If the boundary layer remains unseparated, these mutually induced changes take place in a small interaction region. For a turbulent boundary layer, it has been established [1-8] that an asymptotic description of the interaction region requires a three layer structure. In the outermost layer, comprising most of the boundary layer, pressure forces are much larger than forces resulting from Reynolds or viscous stresses so the governing equations are those for an inviscid flow. For the limit process to be considered, the solutions for this inviscid flow region are those given in Part I of this paper [9], hereafter referred to as (I). Immediately adjacent to the wall is the wall layer, in which viscous and Reynolds stresses dominate to lowest order. Between these two layers is the Reynolds stress sublayer [1] (referred to as the blending layer in reference [2]) in which momentum transfer toward the wall is carried out by turbulent means (Reynolds stresses); the dominant terms in the equation of motion are the Reynolds stress, pressure gradient, and inertia terms.

This paper is concerned with the analysis of the flow in the two inner layers, the Reynolds stress sublayer and the wall layer, the goal being the calculation of the shear stress at the wall in the interaction region. As indicated above, the limit processes considered are those used

in (I). Thus, if ϵ is equal to the nondimensional difference between the velocity and the critical sound speed in the flow external to the boundary layer, and u_T is the nondimensional friction velocity, we consider limit processes such that $u_T \ll \epsilon \ll 1$. In previous analyses for $\epsilon \ll u_T$ (Reference [1]) and $\epsilon = O(u_T)$ (Reference [2]) it was found that it was not possible to formulate an asymptotic criterion for shock induced separation. Here, it will be shown that even for $\epsilon \gg u_T$ there is no apparent asymptotic separation criterion. However, example calculations will be used to show that the equation derived for the wall shear stress may be used to predict conditions for incipient separation with reasonable accuracy.

It is worthwhile reiterating the fact pointed out in (I) that for an unseparated boundary layer the solutions in the inviscid and inner layers are uncoupled. Because the inner layers are so thin, the change in pressure across them is negligible to the order retained and so the solution for the pressure found in the inviscid layer in the limit as the wall is approached is indeed the wall pressure. With this pressure distribution known, then, solutions in the inner layers may be found, leading to a relation for the wall shear stress. Thus, the unseparated flow case is a weak interaction problem. This is not the case for a laminar boundary layer and occurs for the turbulent boundary layer because the wall layer is so thin that the upstream influence of the interaction causes negligible lifting of the fluid from the wall; that is, to the order retained the V component of the velocity is zero, in the

inviscid layer, as the wall is approached. This point will be discussed again later.

In order to complete the formulation of the problem in the inner layers, it is necessary to specify a closure condition. Here, we use a mixing length model, including the van Driest damping factor, to write an eddy viscosity [10]. Such a closure model appears to give satisfactory results as long as the flow is unseparated [11] and has the virtue of simplicity; when the flow is separated, use of such a model gives results which have the correct trends but which do not agree well with experiment.

2. Solutions in the Inner Layers

As in (I), transonic flow over a flat plate with a turbulent boundary layer is considered, with a normal shock wave intersecting the boundary layer; an adiabatic wall is assumed as are conditions such that the total enthalpy may be taken to be uniform throughout the flowfield. Nondimensional Cartesian coordinates X and Y are measured parallel and perpendicular to the wall respectively, with the origin at the point where the normal shock wave intersects the boundary layer. Lengths are made dimensionless with respect to the distance from the leading edge of the flat plate to the shock impingement point, \bar{L} , and Cartesian velocity components U and V with respect to the critical sound speed in the flow upstream of the shock wave and external to the boundary layer (hereafter referred to as the \bar{a}_e^* flow). The

overbars indicate dimensional quantities. The mean temperature, T , density, ρ , pressure, P , and viscosity coefficient, μ , are referred to their critical values in the external flow, e.g., \bar{T}_e^* , \bar{P}_e^* , etc. We write the Reynolds number, Re , in the usual fashion and for convenience define a Reynolds number parameter, Re^* , as follows

$$Re = \left(\frac{\bar{\rho} \bar{U} \bar{L}}{\bar{\mu}} \right)_e \quad (1a)$$

$$Re^* = \left(\frac{\bar{\rho}^* \bar{a}^* \bar{L}}{\bar{\mu}^*} \right)_e \quad (1b)$$

The term $\langle \rho' V' \rangle / \rho$ is included in V , where the primes denote fluctuating quantities and the bracket denotes the average value. The friction velocity, u_τ , is made dimensionless with respect to \bar{a}_e^* , and is defined in terms of the external flow density as follows:

$$u_\tau^2 = \frac{1}{\bar{a}_e^{*2}} \frac{\bar{\tau}_{wu}}{\bar{\rho}_e} = \frac{\bar{\tau}_{wu}}{\bar{\rho}_e} = \frac{1}{2} U_e^2 c_{fu} \quad (2)$$

where $\bar{\tau}_{wu}$ is the shear stress at the wall in the undisturbed flow at $\bar{X} = \bar{L}$, and where c_{fu} is the corresponding skin friction coefficient defined as shown. Finally, the external flow velocity and Mach number are written in terms of a parameter, ϵ , as

$$U_e = 1 + \epsilon \quad (3a)$$

$$M_e^2 = \frac{U_e^2}{1 - \left(\frac{\gamma-1}{2}\right)(U_e^2 - 1)} \quad (3b)$$

ORIGINAL PAGE IS
OF POOR QUALITY

where for transonic flow, $\epsilon \ll 1$. As in (I), the problem considered here is one for which $u_{\tau} \ll \epsilon \ll 1$.

In both inner layers to be considered here, the characteristic thickness of the region is small compared to its characteristic length. As a result, normal Reynolds and viscous stress terms may be neglected compared to the corresponding shear stress terms and the transverse pressure gradient is negligible, to the order retained in the analysis. The solutions to which these inner layer solutions must match in a direction normal to the wall are those solutions found in (I), expanded in the limit as $y = Y/\delta \rightarrow 0$, where $\delta = \bar{\delta}/\bar{L}$ is of the order of the boundary layer thickness. In the limit as $x = X/\Delta \rightarrow -\infty$, where $\Delta = \bar{\Delta}/\bar{L}$ is of the order of the extent of the interaction region, the solutions must match with the corresponding relations in the undisturbed boundary layer. It is seen, then, that the flow problem in the inner layers of the interaction region is formulated as a boundary layer problem with a known pressure gradient. This also helps explain why an additional layer (Reynolds stress sublayer) is necessary in the turbulent boundary layer case. That is, in either the laminar or turbulent interaction, there is an outer layer in the interaction region where pressure forces dominate over shear forces, and inviscid flow equations hold to lower orders. Obviously, then, solutions in the outer layer do not satisfy the no-slip condition at the wall and a new boundary layer must be considered at the wall. In laminar flow, a boundary layer is described asymptotically by a single layer and so only one

so called viscous sublayer is needed in the laminar interaction. However, a turbulent boundary layer has a two layer asymptotic structure; as a result, two inner layers are needed to describe this boundary layer in the interaction region. The Reynolds stress sublayer is the equivalent of the velocity defect layer, as will be seen.

With the above remarks in mind, it is possible to write a simplified set of governing equations in which only those terms needed in either of the two layers considered here are retained. They are as follows:

$$\frac{\partial(\rho U)}{\partial X} + \frac{\partial(\rho V)}{\partial Y} = 0 \quad (4a)$$

$$\rho U \frac{\partial U}{\partial X} + \rho V \frac{\partial U}{\partial Y} = -\frac{1}{\gamma} \frac{\partial P}{\partial X} + \frac{\partial}{\partial Y} (\rho \kappa^2 D Y^2 \left| \frac{\partial U}{\partial Y} \right| \frac{\partial U}{\partial Y}) + \frac{\mu}{Re^*} \frac{\partial U}{\partial Y} \quad (4b)$$

$$\frac{\partial P}{\partial Y} = 0 \quad (4c)$$

$$T + \left(\frac{\gamma-1}{2}\right)U^2 = \frac{\gamma+1}{2} \quad (4d)$$

$$P = \rho T = P(X) \quad (4e)$$

$$D = \left\{ 1 - \exp\left(-\frac{Y Re^* u_\tau}{26}\right) \right\}^2 \quad (4f)$$

where γ is the ratio of specific heats, D is the damping factor, and $\kappa = 0.41$ is the von Kármán constant. Since terms of order u_τ^2 will be retained in the solutions, it should be pointed out that terms such as $\langle \rho' U' \rangle / \rho$ in the continuity equation (4a), and $\langle \rho' T' \rangle$ in the

equation of state, (4e), which are of order u_T^2 , are not included because perturbations from the undisturbed flow values of each of these terms would be of higher than second order. Since the undisturbed flow solutions are considered known to second order, and we are interested only in the perturbations from the undisturbed flow, it is not necessary to include the terms in question. As mentioned previously, it is assumed that the wall is adiabatic, and turbulent and laminar Prandtl numbers are unity, so that the stagnation enthalpy is constant, as in equation (4d).

As shown in (I), for the case $\epsilon/u_T \gg 1$ the distance from the wall to the sonic line is exponentially small compared to the thickness of the boundary layer. Since the extent of the upstream influence of the interaction region is ordered by the thickness of the subsonic region, the upstream influence is confined to a region, hereafter referred to as the inner region, which is exponentially small in the x direction compared to the main part of the interaction region, hereafter referred to as the outer region. That is, in the x direction, the interaction region actually consists of two regions, one thin compared to the other; in the y direction, each of these regions is subdivided into the three layers mentioned previously. Following the procedure employed in (I), the solutions in the outer region will be shown here in some detail. Because the upstream influence is confined to the inner region, the flow entering the shock wave in the outer region is simply the undisturbed flow at the point in question. Inner region solutions,

which are found using precisely the same methods employed in the outer region, are given in reference [12].

Reynolds Stress Sublayer

In the Reynolds stress sublayer, which is intermediate to the outer inviscid flow layer and the wall layer, inertia terms are balanced by both the pressure gradient and Reynolds stress terms in the equation of motion in the flow direction. The extent of the outer interaction region is $X = O(\Delta)$, where, as shown in (I),

$$\Delta = b_o \delta \qquad \delta = O(u_T) \qquad (5a, b)$$

$$b_o = (\gamma+1)^{1/2} \epsilon^{1/2} (1 - (2\gamma+1)\epsilon/4 + \dots) \qquad (5c)$$

If the dimensionless (referred to \bar{L}) thickness of the layer is taken to be $Y = O(\hat{\delta})$, say, then since the Reynolds stress $= O(u_T^2)$ and from (I), $\partial P/\partial X = O(u_T/\Delta)$, the fact that the pressure gradient and Reynolds stress terms in Eqn. (4b) must be of the same order indicates that $\hat{\delta} = O(u_T \Delta)$. Here, for convenience, we define $\hat{\delta}$, \hat{y} and x as follows:

$$\hat{\delta} = u_T \Delta \qquad (6a)$$

$$Y = \hat{\delta} \hat{y} \qquad X = \Delta x \qquad (6b, c)$$

The solutions to which those in the Reynolds stress sublayer must match as $\hat{y} \rightarrow \infty$ are those in the outer inviscid flow layer, written in the limit as $Y/\delta = y \rightarrow 0$. The equations for the U component of velocity and the pressure, (Eqns. (3.9), (3.12), (3.19), (3.21) and (4.2) of (I) are summarized here for convenience. Thus,

$$\begin{aligned}
U(x, 0) = & (1 + \epsilon)^{-1} + u_{\tau} [(1 + 2\gamma\epsilon + \dots)u_{01}(y) \\
& + (1 + (\gamma - 1)\epsilon + \dots)u_1(x)] + \dots \\
& - K\delta \frac{4x}{\pi} \ln(C_0 \delta x) + \dots
\end{aligned} \tag{7a}$$

$$\begin{aligned}
\frac{P_w(x)}{P_e} = \frac{P(x, 0)}{P_e} = & 1 + \gamma(2\epsilon + (2\gamma - 1)\epsilon^2 + \dots) \\
& - u_{\tau}\gamma(1 + (2\gamma - 1)\epsilon + \dots)u_1(x) + \dots \\
& + K\delta \frac{4\gamma x}{\pi} \ln(C_0 \delta x) + \dots
\end{aligned} \tag{7b}$$

$$u_1(x) = -\frac{4x}{\pi} \int_0^{\infty} \frac{u_{01}(\eta)d\eta}{(x^2 + \eta^2)} \tag{7c}$$

where $P_e = 1 - \gamma\epsilon + O(\epsilon^3)$ is the dimensionless pressure in the external flow. The function $u_{01}(y)$ describes the variation of the velocity from its value in the external flow in the velocity defect layer in the undisturbed flow. That is, if U_u represents this velocity component, it may be expanded as

$$U_u = U_e + u_{\tau} u_{01}(y) \tag{8}$$

and $u_{01}(y)$ is the variable part of the velocity distribution in the velocity defect layer in the corresponding incompressible boundary layer [13].

The form given by Coles [14] is used here

$$\begin{aligned}
u_{01}(y) = & \kappa^{-1} [\ln y - \Pi (1 + \cos \pi y)] & 0 < y \leq 1 \\
= & 0 & y > 1
\end{aligned} \tag{9}$$

where Π is Coles' profile parameter. The last terms in Eqns. (7a) and (7b) are due to the curvature of the wall, i.e., for a wall with convex curvature described locally by

$$Y = -\frac{1}{2} K X^2 + \dots \quad (10)$$

where $K \ll 1$ and $K \rightarrow 0$ as $u_\tau \rightarrow 0$ and $\epsilon \rightarrow 0$ such that $K/\epsilon \rightarrow 0$. The value of the constant C_0 is found from the solution for the flow field external to the boundary layer.

If Eqn. (7a) is written in terms of the Reynolds stress sublayer variable, \hat{y} , the result is

$$\begin{aligned} U(x, 0) = & (1 + \epsilon)^{-1} + u_\tau [(1 + 2\gamma\epsilon + \dots) \left(\frac{1}{\kappa} \ln \frac{\hat{\delta}}{\delta} + \hat{u}_{01}(\hat{y}) + \dots \right) \\ & + (1 + (\gamma - 1)\epsilon + \dots) u_1(x)] + \dots \\ & - K\delta \frac{4x}{\pi} \ln(C_0 \delta x) + \dots \end{aligned} \quad (11)$$

where

$$\hat{u}_{01}(\hat{y}) = \kappa^{-1} (\ln \hat{y} - 2\Pi) \quad (12)$$

Thus, equation (11) is the equation to which $U(x, \hat{y})$ must match as $\hat{y} \rightarrow \infty$. As mentioned previously, $\partial P / \partial Y = 0$ to the order retained here. This is easily derived from the equation of motion in the Y direction (e.g., see reference [12]). Hence, the pressure as written in equation (7b) holds throughout both the Reynolds stress sublayer and the thinner wall layer.

In view of the form of equations (11) and (12), the general expansions for U and V are written as follows

$$\begin{aligned}
U(x, \hat{y}) &= (1 + \epsilon)^{-1} + u_{\tau} \left[\frac{1}{\kappa} \ln \frac{\hat{\delta}}{\delta} + \hat{u}_{01}(\hat{y}) + \hat{u}_{11}(x, \hat{y}) \right] \\
&+ \epsilon u_{\tau} \frac{1}{\kappa} \ln \left(\frac{\hat{\delta}}{\delta} \right) \hat{u}_{1\ell}(x, \hat{y}) + \epsilon u_{\tau} \hat{u}_{11}(x, \hat{y}) + \dots \\
&+ \kappa \delta \hat{u}_{1c}(x, \hat{y}; \delta) + \dots
\end{aligned} \tag{13a}$$

$$V(x, \hat{y}) = \hat{v}_1 v_1(x, \hat{y}) + \dots \tag{13b}$$

The corresponding expressions for the temperature, $T(x, \hat{y})$, and density, $\rho(x, \hat{y})$, are found by substituting equation (13a) in the energy equation, (4d) and substituting the resulting expression for the temperature and equation (7b) in the equation of state, Eqn. (4e). If the expansions for U , V , P , and ρ and stretched variables x and y are substituted into Equation (4b), the governing equations for \hat{u}_1 , $\hat{u}_{1\ell}$, and \hat{u}_{11} are found. Thus,

$$\frac{\partial \hat{u}_1}{\partial x} = -\frac{1}{\gamma} \frac{\partial \hat{P}_1}{\partial x} + \frac{\partial}{\partial \hat{y}} \left[(1 + \kappa \hat{y} \frac{\partial \hat{u}_1}{\partial \hat{y}})^2 \right] \tag{14a}$$

$$\frac{\partial \hat{u}_{1\ell}}{\partial x} = \frac{\partial}{\partial \hat{y}} (2\kappa \hat{y} \frac{\partial \hat{u}_{1\ell}}{\partial \hat{y}}) \tag{14b}$$

$$\frac{\partial \hat{u}_{11}}{\partial x} + \gamma \frac{\partial \hat{u}_1}{\partial x} = -\frac{1}{\gamma} \frac{\partial \hat{P}_{11}}{\partial x} + \frac{\partial}{\partial \hat{y}} (2\kappa \hat{y} \frac{\partial \hat{u}_{11}}{\partial \hat{y}}) \tag{14c}$$

$$\frac{\partial \hat{u}_{1c}}{\partial x} = -\frac{1}{\gamma} \frac{\partial \hat{P}_{1c}}{\partial x} + \frac{\partial}{\partial \hat{y}} (2\kappa \hat{y} \frac{\partial \hat{u}_{1c}}{\partial \hat{y}}) \tag{14d}$$

where from Eqn. (7b), \hat{P}_1 , \hat{P}_{11} , and \hat{P}_{1c} are defined as follows

$$\hat{P}_1(x) = -\gamma u_1(x) \tag{15a}$$

$$\hat{P}_{11}(x) = -\gamma (2\gamma - 1) u_1(x) \tag{15b}$$

$$\hat{P}_{1c}(x; \delta) = \frac{4\gamma x}{\pi} \ln(C_0 \delta x) \quad (15c)$$

It should be noted that both \hat{u}_{1c} and \hat{P}_{1c} really denote two terms, one of order $\ln \delta$ and one of order 1. They are written as one here for convenience. Also, it is found [12] that $\hat{v}_1 = O(\epsilon u_\tau^2)$, thus confirming the result used in Part I that, to the order considered here, $V(x, 0) = 0$ in the outer inviscid flow layer.

Insofar as $\hat{u}_1(x, \hat{y})$ is concerned, it is seen from Equation (11) that $\hat{u}_1 \rightarrow u_1(x)$ as $\hat{y} \rightarrow \infty$. It will be shown later that the same functional dependence must hold as $\hat{y} \rightarrow 0$. Since $P_1 = P_1(x)$, the solution which satisfies both matching conditions and the governing equation, (14a), is

$$\hat{u}_1 = \hat{u}_1(x) = \frac{\hat{P}_1(x)}{1} = u_1(x) \quad (16)$$

This result has been used in deriving equations (14b) and (14c). It is easily shown [1, 12] that the solutions to equations (14b)-(14d) may be written as follows

$$\hat{u}_{1f} = 2\gamma + \int_0^x \frac{B_{1f}(\xi)}{(x-\xi)} \exp\left\{-\frac{\hat{y}}{2\kappa(x-\xi)}\right\} d\xi \quad (17a)$$

$$\hat{u}_{1l} = -\gamma \hat{u}_1 - \frac{1}{\gamma} \hat{P}_{1l} + 2\gamma \hat{u}_{0l} + \int_0^x \frac{B_{1l}(\xi)}{(x-\xi)} \exp\left\{-\frac{\hat{y}}{2\kappa(x-\xi)}\right\} d\xi \quad (17b)$$

$$\hat{u}_{1c} = -\frac{\hat{P}_{1c}}{\gamma} + \int_0^x \frac{(B_{1c}(\xi) \ln \delta + B_{1c}(\xi))}{(x-\xi)} \exp\left\{-\frac{\hat{y}}{2\kappa(x-\xi)}\right\} d\xi \quad (17c)$$

where the $B_i(\xi)$ are functions to be found by matching. As $\hat{y} \rightarrow \infty$, the integral terms in each of equations (17) go to zero exponentially and it is seen

that the remaining terms match with their counterparts in equation (11).

As $x \rightarrow 0$, for $\hat{y} = \text{constant}$, the solutions satisfy the shock wave jump conditions to the relevant order, as they should. As $\hat{y} \rightarrow 0$, one finds [1] the following asymptotic behavior for the integrals

$$\int_0^x \frac{B_i(\xi)}{(x-\xi)} \exp\left\{-\frac{\hat{y}}{2\kappa(x-\xi)}\right\} d\xi \sim -B_i(x) \ln\left(\frac{\hat{y}}{2\kappa}\right) + g_i(x) + \dots \quad (18a)$$

$$g_i(x) = \lim_{b \rightarrow 0} \left[\int_0^{x-b} \frac{B_i(\xi)}{(x-\xi)} d\xi + B_i(x) \ln b \right] - \gamma_e B_i(x) \quad (18b)$$

where $\gamma_e = \text{Euler's constant} = 0.57721$.

The solutions for U may thus be found from equation (13a), (16), and (17). Since, as mentioned previously, one can find the density and temperature in terms of the velocity, using the energy equation and the equations of state, it is seen that a complete analytical solution may be found for the Reynolds stress sublayer in the outer region, valid to terms of order ϵu_T . It should be noted that the continuity equation could be used to find the term of order v_1 in V; since it is not used anywhere in this analysis, the solution for V is not included. Finally, it is of interest to write the solution for U in the limit as $\hat{y} \rightarrow 0$ for later use in matching with the wall layer solution. Thus,

$$\begin{aligned}
U = & (1+\epsilon)^{-1} + u_{\tau} [\kappa^{-1} \ln \frac{\hat{\delta}}{\delta} + \hat{u}_{01}(\hat{y}) + u_1(x)] \\
& + \epsilon u_{\tau} \kappa^{-1} \ln \left(\frac{\hat{\delta}}{\delta} \right) [2\gamma - B_{1l}(x) \ln \left(\frac{\hat{y}}{2\kappa} \right) + g_{1l}(x) + \dots] \\
& + \epsilon u_{\tau} [(\gamma-1)u_1(x) + 2\gamma \hat{u}_{01}(\hat{y}) - B_{1l}(x) \ln \left(\frac{\hat{y}}{2\kappa} \right) + g_{1l}(x) + \dots] + \dots \\
& + K\delta \left[-\frac{4x}{\pi} \ln(C_0 \delta x) - (B_{lc}(x) \ln \delta + B_{lc}(x) \ln \left(\frac{\hat{y}}{2\kappa} \right) + g_{lc}(x) \ln \delta \right. \\
& \left. + g_{lc}(x) + \dots \right] + \dots \quad (19)
\end{aligned}$$

Wall Layer

At the wall, Reynolds stresses are zero and the skin friction is, of course, due entirely to viscous stresses. Immediately adjacent to the wall, then, is a layer in which, as the wall is approached, momentum transfer is accomplished less and less by turbulent means and more and more by molecular mechanisms. In this layer, Reynolds and viscous stresses are of the same order. The flow entering the interaction region in this layer has a velocity $U = O(u_{\tau})$ and this order holds in the interaction region as well. If the thickness of the layer is taken to be $Y = O(\tilde{\delta})$, then by equating the orders of the Reynolds and viscous stress terms in equation (4b), one can show that $\tilde{\delta} = O[(Re^* u_{\tau})^{-1}]$. Here, in order to write $\tilde{\delta}$ in terms of familiar quantities, we set

$$\tilde{\delta} = A(Re^* u_{\tau})^{-1} \quad (20a)$$

$$A = \frac{\mu_w}{\mu_e} \left(\frac{T_w}{T_c} \right)^{1/2} U_e \frac{Re^*}{Re} = O(1) \quad (20b)$$

With these orders for Y and U , and since in the interaction region $X = O(\Delta)$ and $\partial P/\partial X = O(u_\tau/\Delta)$, it is seen that, even though a pressure gradient exists, the only terms in equation (4b) are the Reynolds and viscous stress terms, to the order retained. The resulting equation is easily integrated to give

$$\rho D(\tilde{y})(\kappa \tilde{y} \frac{\partial U}{\partial \tilde{y}})^2 + \frac{\mu u_\tau}{A} \frac{\partial U}{\partial \tilde{y}} = u_\tau^2 \rho_e \tau_w \quad (21a)$$

$$\tau_w(x) = \bar{\tau}_w / \bar{\tau}_{wu} \quad (21b)$$

$$Y = \tilde{\delta} \tilde{y} \quad (21c)$$

where, as indicated in Eqn. (21b), the shear stress at the wall, $\tau_w(x)$, is made dimensionless with its value in the undisturbed boundary layer at $\bar{X} = \bar{L}$, so that as $x = X/\Delta \rightarrow -\infty$, $\tau_w \rightarrow 1$. Equation (21a) is essentially the same equation used in references [1] and [2]; the only difference lies in the closure conditions used.

With the orders mentioned above for U , P , X , and Y , and for $\rho = O(1)$, it is easy to show [12] that $V = O(u_\tau \tilde{\delta}/\Delta)$ and to corroborate equation (4c) to the order retained. Since $U = O(u_\tau)$, then from the energy equation, (4d), it is seen that $T = T_w + O(u_\tau^2)$ and from the equation of state, equation (4e), then, that variations in ρ in the Y direction are also $O(u_\tau^2)$. Hence, to order u_τ^2 , $\rho = \rho_w$ and as pointed out previously by Melnik and Grossman [2] and Adamson and Feo [1], the fact that $\rho_w \neq \rho_e$ leads to the result that limit process expansions in the wall layer do not match with corresponding expansions from the Reynolds stress sublayer; thus, this

difficulty arises only in compressible flow. The difficulty may be overcome by taking advantage of the range of validity of equation (21a). That is, in any intermediate limit $\tilde{\delta} \ll Y \ll \hat{\delta}$, equation (21a) is still the governing equation; it is necessary to retain additional terms only for $Y = O(\hat{\delta})$. Hence equation (21a) may be used to derive solutions which will match with those found using limit process expansions in either limit, $Y = O(\hat{\delta})$ or $Y = O(\tilde{\delta})$. Although the methods of solution used by Adamson and Feo and Melnik and Grossman are equivalent, the latter's method is more straightforward and will be used here.

It is clear both from physical arguments, and from consideration of equation (21a) that as Y increases such that $\tilde{y} \gg 1$, the viscous terms become negligible compared to the Reynolds stress terms; this is borne out by using the solution to be derived to compare the two terms. Also, for $\tilde{y} \gg 1$, the damping factor D is represented by unity plus exponentially small terms (eqn. 5). Finally, the density may be written in terms of the velocity and pressure, in general, by using equations (4e) and (4d). Since $P = P(x)$ to the order retained, equation (21a) may be integrated to give,

$$U(x, \tilde{y}) = \Gamma \sin \left\{ \frac{1}{\Gamma} \left(\frac{T_w}{T_e} \right)^{1/2} \left(\frac{T_w}{P_w/P_e} \right)^{1/2} u_{\tau k} \left(\frac{1}{\tau k} \ln \tilde{y} + B(x) \right) \right\} \quad (22a)$$

$$\Gamma = \sqrt{\frac{\gamma+1}{\gamma-1}} \quad (22b)$$

where $T_w = (\gamma+1)/2$ is the temperature at the wall and T_w/T_e can be found in terms of U_e from the energy equation, (4d). $B(x)$ is a function of integration which should be evaluated by matching equation (22a) with the

limit process expansion solution valid in the wall layer ($\tilde{y} = O(1)$); that is, it should be found as a result of integration from the wall to the \tilde{y} value in question, using the boundary conditions at the wall. However, it is only necessary to evaluate $B(x)$ to lowest order here, and this may be done by noting that if there were no shock wave, then $B(x) = C$, the constant from the undisturbed flow wall layer solution (eqn. (2.8), in (I)). Here, then, $B(x)$ is written in terms of an asymptotic expansion

$$B(x) = C + \omega(u_T) B_1(x) + \dots \quad (23)$$

where $\omega(u_T) \rightarrow 0$ as $u_T \rightarrow 0$.

Since equations (22a) must match with equation (19), in the limit as $\tilde{y} \rightarrow \infty$, $\hat{y} \rightarrow 0$, it is seen that τ_w must have an expansion of the following form

$$\begin{aligned} \tau_w(x) = & 1 + a_1 \epsilon + a_2 \epsilon^2 + \dots + u_T \tau_1(x) + \epsilon u_T \frac{1}{\kappa} \ln\left(\frac{\hat{\delta}}{\delta}\right) \tau_{1f}(x) \\ & + \epsilon u_T \tau_{1l}(x) + \dots + K\delta \tau_{1c}(x) + \dots \end{aligned} \quad (24)$$

That is, as $\tilde{y} \rightarrow \infty$, such that $u_T \kappa^{-1} \ln \tilde{y} = O(1)$,

$$u_T \ln \tilde{y} = u_T \ln \frac{\hat{\delta}}{\delta} + u_T \ln \frac{\delta}{\tilde{\delta}} + u_T \ln \hat{y} \quad (25)$$

where, as shown in (I) (equation (2.9))

$$\frac{u_T}{\kappa} \ln \frac{\delta}{\tilde{\delta}} = \left(\frac{T_e}{T_w}\right)^{1/2} \Gamma \sin^{-1}\{U_e/\Gamma\} - u_T \left(\frac{2\Pi}{\kappa} + C\right) \quad (26)$$

and the expansion for τ_w shown in equation (24) follows to insure the indicated matching. Thus, if equation (7b), (23), (24), (25), and (26) are substituted into equation (22a) and the resulting equation is compared with

equation (19) term by term, the unknown parameters and functions in equations (24) and (19) may be found. The resulting solution for τ_w , the shear stress at the wall in the outer interaction region, and the corresponding values for the B_i and g_i (calculated once the B_i are known using equation (18b)) in equation (19) are

$$\begin{aligned}
\tau_w(x) = & 1 + a_1 \epsilon + \frac{a_1(a_1-1)}{2} \epsilon^2 + \dots - u_\tau \frac{a_1}{2} u_1(x) \\
& + \epsilon u_\tau \kappa^{-1} \ln\left(\frac{\delta}{\delta}\right) (2\gamma - a_1) \left(\gamma + \frac{1}{2} - \frac{a_1}{4}\right) \\
& + \epsilon u_\tau \left\{ u_1(x) \left[\frac{a_1}{4} (1 - 3\gamma - \frac{3a_1}{2}) + \gamma(\gamma + \frac{1}{2}) \right] \right. \\
& - 2\pi \kappa^{-1} (2\gamma - a_1) \left(\gamma + \frac{1}{2} - \frac{a_1}{4}\right) \\
& \left. + \kappa^{-1} (2\gamma + 1 - \frac{a_1}{2}) \left(\gamma - \frac{a_1}{2}\right) (\ln x - \gamma_e + \ln 2\kappa) \right\} + \dots \\
& + K \delta \frac{2a_1 x}{\Pi} \ln(C_o \delta x) + \dots
\end{aligned} \tag{27a}$$

$$a_1 = -4 \sqrt{\frac{\gamma-1}{2}} \left(\sin^{-1} \frac{1}{\Gamma}\right)^{-1} + 2\gamma \tag{27b}$$

$$B_{1l} = g_{1l} = 0 \tag{27c}$$

$$B_{11} = \kappa^{-1} \left[2\gamma + 1 - \frac{a_1}{2} \right] \tag{27d}$$

$$g_{11} = B_{11} (\ln x - \gamma_e) \tag{27e}$$

where $u_1(x)$ is given in equation (7c). Equation (27a), then, is the solution for $\tau_w(x)$ in the interaction region, including the effects of curvature in the external flow field. It has, in most respects, the same form as the equation

derived by Melnik and Grossman [2], differing mainly in the order of the various terms, the inclusion of specific analytical solutions at each order of approximation, and the inclusion of the curvature terms.

The order to make numerical calculations for a given Reynolds number, Re , and external flow Mach number, $M_e = 1 + (\gamma+1)\epsilon/2 + \dots$, it is necessary to provide relations for u_τ and δ in terms of Re and ϵ . One of the required equations is equation (26), with equations (20) for $\tilde{\delta}$; the other is given in (I), (eqn. (2.11), 2.12)). This equation, with the values of the integrals as given by Cebeci and Smith [10] is repeated here for completeness.

$$\delta = \frac{u_\tau}{U_e} \frac{\kappa}{(1+\Pi)} + \left(\frac{u_\tau}{U_e}\right)^2 \left\{ \frac{2}{(1+\Pi) \sin^{-1}\left(\frac{U_e}{\Gamma}\right)} \frac{U_e}{\Gamma} \left(1 - \frac{U_e^2}{\Gamma^2}\right)^{-1/2} + \frac{1}{2} \left(\frac{1}{(1+\Pi)^2} \frac{[2 + (U_e/\Gamma)^2]}{[1 - (U_e/\Gamma)^2]} (2 + 3.1787\Pi + \frac{3}{2}\Pi^2) \right) \right\} \quad (28)$$

where $T_e/T_w = 1 - (U_e/\Gamma)^2$ from the energy equation, (4d). Finally, it is necessary to write an equation for the viscosity, $\mu(T)$, to be used in equations (20).

Here, $\mu = T^n$ was used, with calculations being performed for $n = 3/4$.

Finally, it should be noted that although the solutions presented here are found to orders of approximation such that pressure gradient and inertia terms were not retained in the equation of motion in the wall layer, higher order solutions involving these terms have been investigated [12]. It was found that the first terms to involve the pressure gradient were of order $\tilde{\delta}/\Delta$ in U and of order $\tilde{\delta}/u_\tau \Delta$ in τ_w . Thus, they give very small corrections to the solutions presented.

3. Numerical Calculations and Separation Criterion

The variation of τ_w with x for various values of external flow Mach number (and thus ϵ) and Reynolds numbers representative of modern aircraft are shown in figure 1. The numerical computations were carried out using equations (27a) for $\mu = T^{3/4}$, $\gamma = 1.4$, $\Pi = 1/2$, $C = 5$ and $K = 0$; these values seem to be suitable for flow over a flat plate. The curves show the general features found experimentally in the interaction region. That is, $\tau_w(x)$ goes through a minimum, say $(\tau_w)_{\min}$; as M_e increases, $(\tau_w)_{\min}$ decreases, while as Re increases $(\tau_w)_{\min}$ increases. Thus, the effect of increasing M_e and therefore the strength of the shock wave is to decrease the value of τ_w everywhere in the interaction region and hence to force the flow toward separation; increasing Re gives the opposite effect. It should be noted that $\tau_w \rightarrow 1$ as $x \rightarrow 0$ because the solution shown in Eqn. (27a) is for the outer interaction region. A solution for τ_w valid in the inner region can be written in terms of the solutions for the pressure perturbations in the inner inviscid flow region [12]; The solution is found in precisely the same manner as that illustrated here for the outer region and results in a solution similar to that given in Eqn. (27a). Finally, a composite solution for τ_w could be written, using the solutions valid in the inner and outer regions. Because of the limit processes considered in this work ($\epsilon \gg u_T$), this composite solution would show only a small variation in τ_w for $x < 0$. However, since analytical solutions cannot be obtained for the pressure in the inner region, no solution for τ_w in the inner region has been included here:

It is not possible to compare the solution for τ_w with experimental results

for a completely two dimensional unseparated flow because none are available. In those cases where the flow was apparently unseparated (e. g., references [15, 16]), τ_w was not measured, and in more recent work, where τ_w has been measured (e. g., references [17, 18, 19]) the flow is separated. In separated flow, the shock wave takes on a lambda configuration near the boundary layer and a relatively strong pressure gradient develops in the Y direction in the flow external to the boundary layer [18]; the flow picture is quite different from the unseparated flow case considered here.

Although experimental results for truly two dimensional flow are not available for comparison, there is one set of measurements in a tube in which the flow is approximately two dimensional [20]. Thus, if R is the dimensionless (with respect to \bar{L}) radius of the tube, $\delta/R \cong 0.04$ to 0.08 ; in addition, the changes in the core flow (external to the boundary layer) due to the rapid increase in the boundary layer displacement thickness through the interaction region give corrections which are asymptotically of higher order than those retained in Eqn. (27a). In presenting the tube data, Gadd fitted power law velocity profiles to the measured profiles and inferred values of $\bar{\delta}$ (dimensional boundary layer thickness) immediately upstream of the interaction. Using equations derived using power law profiles, he also gave Reynolds numbers associated with the tunnel stagnation pressure and Mach number for each test. Skin friction measurements were derived from Stanton tube measurements. In determining the flow parameters to be used in calculating τ_w for comparison with each of Gadd's experiments, it was decided to use Gadd's values of $\bar{\delta}$, Re , M_e , and stagnation pressure, \bar{P}_{te} as being a self-

consistent set of data to calculate the necessary ϵ , u_τ , δ , and Π for use in τ_w . Thus, it is easy to show that if $\mu = T^n$,

$$\text{Re } \delta = \frac{\bar{P}_t}{\bar{P}_{at}} \frac{M_e}{\left[1 + \frac{\gamma-1}{2} M_e^2\right]^{\frac{\gamma}{\gamma-1}}} \left(1 - \frac{U_e^2}{\Gamma^2}\right)^{-n-1/2} \frac{\bar{a}_w \bar{\delta}}{\bar{v}_w} \quad (29)$$

Here, \bar{a}_w and \bar{v}_w are the dimensional speed of sound and kinematic viscosity respectively, evaluated at the wall temperature (atmospheric temperature, taken to be 59°F.) and in the case of \bar{v}_w , at atmospheric sea level density; \bar{P}_{at} refers to atmospheric pressure. Using the given values of M_e , \bar{P}_t , $\bar{\delta}$, and $\bar{\tau}_w$, Eqns. (3), (26), (with Eqn. (20) for $\bar{\delta}$), (28) and (29) were used to calculate the equivalent ϵ , u_τ , δ , and Π . From equation (2), then, the corresponding c_{fu} could be calculated. The ratio of the calculated C_{fu} to the value inferred from the standard tube measurements ranged from 1.05 to 1.29 in four cases reported by Gadd (Figures 25 to 28, reference [20]). For this reason and because of uncertainties in the calibration of the Stanton tube, it was decided to compare values of c_f/c_{fu} , which is equal to τ_w as given in equation (27a). The results of this comparison are shown in figure 2, for the case $M_e = 1.15$, $\text{Re} = 7 \times 10^6$, (Figure 25, reference [20]). The remaining parameters are given under figure (2). The point $X'/\delta = 0$, defined by Gadd as the position at which $P_w/P_{te} = 0.528$, was found by using equation (7b). It is seen that the measured upstream influence is not small. That is, c_f/c_{fu} is not small for $X < -1$ say, as required for this theory, so that even if the solution for τ_w for $x < 0$ were available, it is not expected that it would give good agreement. In fact, using the above mentioned parameters,

$\delta_*/\delta = 0.5$, where δ_* is the dimensionless distance to the sonic line in the undisturbed boundary layer; evidently the values for Re , ϵ , and Π do not form a good combination for comparison with the theory. On the other hand, a slight unsteadiness in the position of the shock wave could have contributed to the slow variation of the measured c_f/c_{fu} upstream of and in the neighborhood of the minimum. Nevertheless, the value and the position of the minimum of c_f/c_{fu} are predicted quite accurately. Downstream of the minimum the comparison is fairly good; in this regard, however, it is interesting to note that the negative curvature seen on the calculated curve but not on this particular experimental curve, is a feature found in other experimental results which could not be used here because small separation bubbles existed.

It is of interest at this point to consider the problem of predicting conditions under which the interaction brings the flow to the point of incipient separation. First, it is seen from equation (27a) that there is no asymptotic condition for incipient separation; that is, unlike the laminar case, in which $\epsilon_s = O(Re^{-1/5})$ is the asymptotic criterion [21], there is no relation between ϵ and Re which holds in the limit as $Re \rightarrow \infty$ as a condition for separation. This is an important difference between the two flows, and it is of interest to investigate the reason for its occurrence. The effect of the interaction, through the induced adverse pressure gradient, is to slow the fluid. In the boundary layer, then, the stream tubes must become wider and, due to the constraint of the wall, the V velocity component increases at points away from the wall, causing the outer flow to lift away from the wall also. In the laminar case, the thickening of streamtubes is greatest in the viscous sublayer.

The resulting V component of velocity is large enough that the flow external to the boundary layer is affected to lowest order so that the external and boundary layer flows must be considered simultaneously, i. e., a strong interaction results [21, 22]. No matter how large Re becomes, this strong interaction occurs, with the thickness of the viscous sublayer and boundary layer decreasing as Re increases, according to their asymptotic dependence on Re . The sublayer momentum flux and viscous stresses decrease and the strength of the shock wave necessary to cause enough displacement of the fluid to result in separation decreases as Re increases. In the turbulent case, even for $\epsilon \gg u_\tau$, the interaction is a weak interaction to lowest order because the wall layer is so thin. Thus, until separation occurs, the outward displacement of the fluid in the wall layer due to the interaction is too small to cause any effect in the lowest order solutions in the flow external to the boundary layer. A strong interaction does not occur until a separation bubble exists. Since there is no mechanism through which variations in the wall layer and external flows can interact, before a separation bubble is formed, it appears that no asymptotic criterion exists for incipient separation. However, it may be that such a criterion will result from an asymptotic solution for the separated flow problem in the limit as the size of the bubble shrinks to zero.

Although the solution for $\tau_w(x)$ does not give an asymptotic criterion for separation, there remains the possibility that conditions for incipient separation can be found simply by assuming that equation (27a) is an accurate solution for $\tau_w(x)$ at values of M_e and Re near separation. It is

clear from figures 1 and 2 that the solution shows the correct form with a minimum value, and it is possible to calculate the corresponding values of Re and M_e (i. e., ϵ) for which $(\tau_w)_{\min} = 0$, the condition for incipient separation. It must be emphasized that equation (27a) is not being used in an asymptotic sense in such a calculation; thus in order for τ_w to go to zero, one or more terms in the expansion must become as large as the first term. Instead, we consider equation (27a) as being a good approximation to $\tau_w(x)$ in a numerical sense as long as ϵ^3 and u_τ^2 (the orders of the first terms neglected) are small compared to one.

To illustrate the use of equation (27a) for $\tau_w(x)$ to predict conditions for separation, we choose the remainder of Gadd's tubes flow experiments in which c_f was measured [20]. That is, Gadd presented four plots of c_f vs. X'/δ (Figures 25-28, reference [20]), the first of which is shown in figure 2. In each case he also performed oil-flow experiments, which indicated that in one case (used in figure 2) the flow was not separated, but that in the three other cases, separation did occur. Although the plotted values of c_f did not indicate the occurrence of separation in these three cases, it should be noted that the values of c_f were inferred from measurements from a Stanton tube aligned facing the flow; thus, accurate reverse flow measurements could not be made. Calculations of τ_w were made for each of these cases, using the same method for calculating the necessary parameters, as mentioned in the discussion of figure 2. The resulting values for $(\tau_w)_{\min} = (c_f/c_{fu})_{\min}$ for each case are as follows:

$$\begin{array}{lll}
(1) & M_e = 1.27 & Re = 10^7 & (\tau_w)_{\min} = -0.080 \\
(2) & M_e = 1.26 & Re = 1.27 \times 10^7 & (\tau_w)_{\min} = -0.020 \\
(3) & M_e = 1.34 & Re = 1.93 \times 10^7 & (\tau_w)_{\min} = -0.344
\end{array}$$

Thus these calculated results indicate that in all three cases the flow is separated, in agreement with the oil-flow experiments. In case (2), the extent of the region where $\tau_w < 0$, i. e., the extent of the separation bubble, appears to be very small; the flow is barely separated.

If we denote by M_{es} the Mach number of the external flow at incipient separation, equation (27a) may be used, with the condition that $(\tau_w)_{\min} = 0$, to find M_{es} as a function of Re . A typical result is shown in figure (3) for $K = 0$ and $\Pi = 1/2$, i. e., for conditions associated with flow along a flat plate. It is seen that according to this prediction, M_{es} increases as Re increases. This result is in agreement with measurements made by Roshko and Thomke [23] for supersonic flow at high Reynolds numbers. The magnitude of the increase in M_{es} over a large range of Re , however, is small enough that this result could help explain the conclusion that there was little or no variation with Re , reached by Settles, Bogdonoff, and Vas [24].

The effects of curvature on M_{es} , as predicted by equation (27a) can also be compared with experimental results. Evidently, the only data available are those presented in figure (37) of reference [20], reproduced here as figure 4. The value of the coordinate along the abscissa, t , is given as $t \approx 2.6 \delta / R$ where R is the radius of curvature; in view of equation (10), then, one can write $t = 2.6\delta K$. Although there is no dependence on Reynolds number shown, it is assumed here that the range of Reynolds numbers is

10^6 to 10^7 and calculated results are given for both values. Finally, on an airfoil with supercritical flow, the flow is accelerating up to the shock wave; since Π depends on the pressure gradient in the undisturbed flow upstream of the interaction, the value of Π on an airfoil will be different for different curvatures. For zero pressure gradient $\Pi \cong 0.5$, whereas for highly accelerating flow Π is smaller and can become negative [25]. Therefore, at $t = 0$, $\Pi \cong 0.5$, ($K = 0$) and at $t = 0.015$, it was decided to use a value of Π for moderately accelerated flows, $\Pi = 0$. The values of M_{es} at $t = 0$ can be found from figure (3). Those at $t = 0.015$, for which $K = 0.021$ at $Re = 10^6$ and $K = 0.028$ at $Re = 10^7$, were calculated, again using equation (27a). The results are shown in figure (4). It is seen that at the conditions associated with flow over a flat plate ($t=0$) the calculated M_{es} compares very well with the value given by the line drawn through the experimental data. On the other hand, at higher curvature ($t = 0.015$) the calculated values are considerably less than those found experimentally. In reference [20] there was some discussion of the fact that criteria for separation might have been too stringent in the curved surface cases so that, for example, the point through which the drawn line passes at $M_{es} = 1.31$ perhaps should have been at $M_{es} = 1.29$. If this were the case and if negative values of Π were called for, the agreement at $t = 0.015$, would be much better.

The present results for criteria for shock induced incipient separation may be compared with theoretical predictions given by Bohning and Zierrep [26], who postulated a two layer model for the interaction region and were able to calculate an equation for c_f . Two comparisons were made, both for

flat plates, at Re values of 10^6 and 5×10^6 ; these Re are in the range of results presented in reference [26]. At $Re = 10^6$, the predicted values of M_{es} are 1.24 and 1.18 and at $Re = 5 \times 10^6$ they are 1.26 and 1.30, where the M_{es} calculated by the present method is the first, in each case. Thus, although the two solutions give the same M_{es} at some Re between 10^6 and 5×10^6 , Bohning and Zierep's solution shows a much greater variation of M_{es} with Re than that shown here. However, the present results appear to be in closer agreement with experimental measurements [23, 24] for a related problem. The present theory could not be compared with very recent analytical results given by Inger [27], who also used a two layer model, since conditions for incipient separation were not presented.

Although there appears to be no asymptotic criterion for separation in the limit as $Re \rightarrow \infty$ ($u_\tau \rightarrow 0$) and $\epsilon \rightarrow 0$, there remains the possibility that there exists a criterion involving a large M_e as $Re \rightarrow \infty$. Thus, it is necessary to consider the behavior of τ_w for $\epsilon = O(1)$. Based on the present analysis, it is seen that for $\epsilon = O(1)$, $u_\tau \ll 1$, the solution for $\tau_w(x)$ would be of the following form in the outer interaction region:

$$\tau_w(x) = \tau_{w_d}(\epsilon) + u_\tau \tau_{w_1}(x; \epsilon) + \dots \quad (30)$$

where $\tau_{w_d}(\epsilon)$ is the value which $\tau_w(x)$ approaches far downstream of the shock wave. Since the lowest order solutions for the velocities would be of the same form in each of the layers as for $\epsilon \ll 1$, it is seen that, from matching solutions in the limit $u_\tau \rightarrow 0$, one would obtain

$$\Gamma \sin \left\{ \left(\frac{\tau_{w_d}}{P_d/P_e} \right)^{1/2} \sin^{-1} \left(\frac{U_e}{\Gamma} \right) \right\} = U_d \quad (31)$$

Here P_d and U_d are the values of P and U immediately downstream of the shock wave in the inviscid flow external to the boundary layer respectively, and are thus the values which P and U approach as $x \rightarrow \infty$ in the interaction region. If the jump conditions across a shock wave are used to write U_d and P_d/P_e in terms of U_e and these expressions are substituted into equation (31), one obtains an expression for τ_{w_d} in terms of U_e . Thus,

$$\tau_{w_d} = \left[\frac{1 + \left(\frac{\gamma+1}{2}\right)(U_e^2 - 1)}{1 - \left(\frac{\gamma-1}{2}\right)(U_e^2 - 1)} \right] \left[\frac{\sin^{-1}\left(\frac{1}{\Gamma U_e}\right)}{\sin^{-1}\left(\frac{U_e}{\Gamma}\right)} \right]^2 \quad (32)$$

If $U_e = 1 + \epsilon$ is substituted into equation (32) and the resulting equation expanded for $\epsilon \ll 1$, it is found that $\tau_{w_d} = 1 + a_1\epsilon + a_1(a_1 - 1)\epsilon^2/2 + \dots$, in agreement with the first three terms of equation (27a).

It is clear from equation (32) that, since $1 \leq U_e < \Gamma$ for $1 \leq M_e < \infty$ (see eqn. (36)), $\tau_{w_d} \neq 0$ for any M_e ; instead τ_{w_d} goes through a minimum value of 0.512 at $M_e = 2.55$, for $\gamma = 1.4$, and then begins to rise with increasing M_e . Hence, there is apparently no limiting value for M_{es} as $Re \rightarrow \infty$. Moreover, since $U_e \rightarrow \Gamma$ as $M_e \rightarrow \infty$, it is clear that $\tau_{w_d} \rightarrow \infty$. Recalling the definition of $\tau_w(x)$, one can see that this limit means that for high Mach number flow the shear stress far downstream of the interaction must be large compared to that of the undisturbed flow. This apparent anomaly can be explained by considering equation (21a). The density, in the first term, can be written as P/T through the equation of state. Now, in the wall layer, the temperature differs from the constant temperature of the wall by only higher order terms. On the other hand, since $\partial P/\partial Y = 0$

through the wall layer and Reynolds stress sublayer, P is the pressure from the inviscid flow layer and so varies from P_e to P_d . As $M_e \rightarrow \infty$, $P_d/P_e \rightarrow \infty$ and so from equation (21a), $\tau_{wd} \rightarrow \infty$ also. In general, since the Reynolds shear stress, $-\rho \langle U' V' \rangle$, includes the density, this result appears to be independent of the specific closure condition as long as $\langle U' V' \rangle$ does not go to zero as $M_e \rightarrow \infty$, and is another significant departure from the laminar case. Experimental verification of the large values of τ_{wd} at high Mach numbers is given in measurements by Marvin, et al. [28].

4. Concluding Remarks

The use of asymptotic methods of analysis results in a relatively simple relation for the shear stress at the wall in the interaction region. This relation may be used to predict conditions for incipient separation. In order to obtain the proper variation of τ_w vs. x , which includes a minimum in τ_w , it is necessary to include terms of higher order than the first approximation; evidently this would be the case also if one were to calculate τ_w for the case $u_T = O(\epsilon)$ [2].

Although the range of parameters in available experiments does not allow for exhaustive testing of the theory, comparisons which could be made are encouraging; more accurate results should be obtained at the high Reynolds

numbers associated with modern transonic aircraft.

Acknowledgement

Support for this work, by NASA Langley Research Center, Grant NSG 1326, is gratefully acknowledged. The authors wish to thank Professor A. F. Messiter for his many helpful suggestions during the course of this work and Dr. R. Enlow, University of Otago, Dunedin, New Zealand, for his help in performing numerical calculations.

References

- [1] T. C. Adamson, Jr. and A. Feo, "Interaction Between a Shock Wave and a Turbulent Boundary Layer in Transonic Flow," *SIAM J. Appl. Math.*, **29**, 121-145 (1975).
- [2] R. E. Melnik and B. Grossman, "Analysis of the Interaction of a Weak Normal Shock Wave with a Turbulent Boundary Layer," *AIAA Paper No. 74-598* (1974).
- [3] R. E. Melnik and B. Grossman, "Further Developments in an Analysis of the Interaction of a Weak Normal Shock Wave with a Turbulent Boundary Layer," *Symposium Transsonicum II*, K. Oswatitsch and D. Rues, eds., Springer-Verlag, 262-272 (1976).
- [4] T. C. Adamson, Jr., "The Structure of Shock Wave Boundary Layer Interactions in Transonic Flow," *Symposium Transsonicum II*, K. Oswatitsch and D. Rues, eds., Springer-Verlag, 244-251 (1976).
- [5] R. E. Melnik and B. Grossman, "Interaction of Normal Shock Waves with Turbulent Boundary Layers at Transonic Speeds," *Transonic Flow Problems in Turbomachinery*, T. C. Adamson, Jr. and M. F. Platzer, eds., Plenum Press, 415-433 (1977).
- [6] T. C. Adamson, Jr. and A. F. Messiter, "Normal Shock Wave-Turbulent Boundary Layer Interactions in Transonic Flow Near Separation," *Transonic Flow Problems in Turbomachinery*, T. C. Adamson, Jr. and M. F. Platzer, eds., Plenum Press, 392-414 (1977).
- [7] T. C. Adamson, Jr. and A. F. Messiter, "Shock Wave-Turbulent Boundary Layer Interactions in Transonic Flow," *Advances in Engineering Science*, NASA CP-2001, 1425-1435 (1976).

- [8] A. F. Messiter and T. C. Adamson, Jr., "A Study of the Interaction of a Normal Shock Wave with a Turbulent Boundary Layer at Transonic Speeds," NASA Conference on Advanced Technology Airfoil Research, Vol. I, NASA Conf. Publ. 2045, 271-279 (1978).
- [9] A. F. Messiter, "Interaction Between a Normal Shock Wave and a Turbulent Boundary Layer at High Transonic Speed, Part I; Pressure Distribution," submitted for publication.
- [10] T. Cebeci and A. M. O. Smith, "Analysis of Turbulent Boundary Layers," Academic Press (1974).
- [11] J. R. Viegas and T. J. Coakley, "Numerical Investigation of Turbulence Models for Shock-Separated Boundary Layer Flows," AIAA J., 16, 293-294 (1978).
- [12] M. S. Liou, "Asymptotic Analysis of Interaction between a Normal Shock Wave and a Turbulent Boundary Layer in Transonic Flow," Ph.D. Dissertation, The University of Michigan, Ann Arbor, Michigan (1977).
- [13] G. Maise and H. McDonald, "Mixing Length and Kinematic Eddy Viscosity in a Compressible Boundary Layer," AIAA J., 6, 73-80, (1968).
- [14] D. E. Coles, "The Law of the Wake in the Turbulent Boundary Layer," J. Fluid Mech., 42, 411-427 (1970).
- [15] J. Ackeret, F. Feldmann and N. Rott, "Untersuchungen an Verdichtungsstößen und Grenzschichten in Schnell Bewegten Gasen," Mitteilungen aus dem Inst. für Aerodyn., ETH Zürich, Nr 10 (1946). Translated as NACA TM 1113 (1947).

- [16] H. W. Liepmann, "Interaction Between Boundary Layers and Shock Waves in Transonic Flow," J. Aero. Sci., 13, 623-637 (1946).
- [17] R. J. Vidal, C. E. Wittliff, P. A. Catlin and B. H. Sheen, "Reynolds Number Effects on the Shock Wave-Turbulent Boundary Layer Interaction at Transonic Speeds," AIAA Paper No. 73-661 (1973).
- [18] J. W. Kooi, "Experiment on Transonic Shock-Wave Boundary-Layer Interaction," NLR MP 75002 U, National Aerospace Laboratory, The Netherlands (1975).
- [19] G. G. Mateer, A. Brosh, and J. R. Viegas, "A Normal Shock-Wave Turbulent Boundary-Layer Interaction at Transonic Speeds," AIAA Paper No. 76-161 (1976).
- [20] G. E. Gadd, "Interaction Between Normal Shock Waves and Turbulent Boundary Layers," A.R.C. 22559, R. and M. 3262 (1962).
- [21] A. F. Messiter, A. Feo and R. E. Melnik, "Shock Wave Strength for Separation of a Laminar Boundary Layer at Transonic Speeds," AIAA J., 9, 1197-1198 (1971).
- [22] H. M. Brilliant and T. C. Adamson, Jr., "Shock Wave Boundary Layer Interactions in Laminar Transonic Flow," AIAA J., 12, 323-329 (1974).
- [23] A. Roshko and G. J. Thomke, "Supersonic Turbulent Boundary-Layer Interaction with a Compression Corner at Very High Reynolds Number," Proceedings of the 1969 Symposium, Viscous Interaction Phenomena in Supersonic and Hypersonic Flow, University of Dayton Press, 109-138 (1970).

- [24] G. S. Settles, S. M. Bogdonoff and I. E. Vas, "Incipient Separation of a Supersonic Turbulent Boundary Layer at High Reynolds Numbers," AIAA J., 14, 50-56 (1976).
- [25] J. E. Lewis, R. L. Gran and T. Kubota, "An Experiment on the Adiabatic Compressible Turbulent Boundary Layer in Adverse and Favorable Pressure Gradients," J. Fluid Mech., 51, 657-672 (1972).
- [26] R. Bohning and J. Zierep, "Bedingung Für Das Einsetzen Der Ablösung Der Turbulenten Grenzschicht an Der Gekrümmten Wand Mit Senkrechtem Verdichtungsstoss," ZAMP, 29, 190-198 (1978).
- [27] G. R. Inger, "Transonic Shock-Turbulent Boundary Layer Interaction with Suction and Blowing," AIAA Paper No. 79-0005 (1979).
- [28] J. G. Marvin, C. C. Horstman, M. W. Rubesin, T. J. Coakley and M. I. Kussoy, "An Experimental and Numerical Investigation of Shock-Wave Induced Turbulent Boundary-Layer Separation at Hypersonic Speeds," Flow Separation, AGARD CP-168, 25-1 to 25-13, November (1975).

Figure Titles

- Figure 1 τ_w vs x for various values of Me and Re , for flow over a flat plate. (Eqn. (27a) with $\Pi = 0.5$, $K = 0$).
- Figure 2 Comparison of calculated (eqn. (27a)) and experimental (ref. [20]) values of c_f/c_{fu} vs X'/δ . Experimental conditions; $Me = 1.15$, $Re = 7 \times 10^6$, wall temperature = $15^\circ C$ ($59^\circ F$), $\bar{P}_{te} = 137.9 \text{ kPa gauge}$ (20 psig), $\bar{\delta} = 0.305 \text{ cm}$ (0.12 in). Corresponding calculated parameters; $\epsilon = 0.120$, $u_T = 0.03968$, $\delta = 0.01634$, $\Pi = 0.312$, $K = 0$. $X'/\delta = 0$ at $P_w/P_{te} = 0.528$ from eqn. (7a).
- Figure 3 M_{es} (Mach number at incipient separation) vs Re for flow over a flat plate, calculated using eqn. (27a) with $(\tau_w)_{min} = 0$, $\Pi = 0.5$, $K = 0$.
- Figure 4 Effect of curvature parameter, t , on Mach number for incipient separation, M_{es} , from Reference [20]. Triangles and circles correspond to different airfoils. Present calculations shown as follows: at $t = 0$, \blacksquare - $Re = 10^6$, $\Pi = 0.5$, $K = 0$; \times - $Re = 10^7$, $\Pi = 0.5$, $K = 0$. At $t = 0.015$, \blacksquare - $Re = 10^6$, $\Pi = 0$, $K = 0.21$; \times - $Re = 10^7$, $\Pi = 0$, $K = 0.28$.

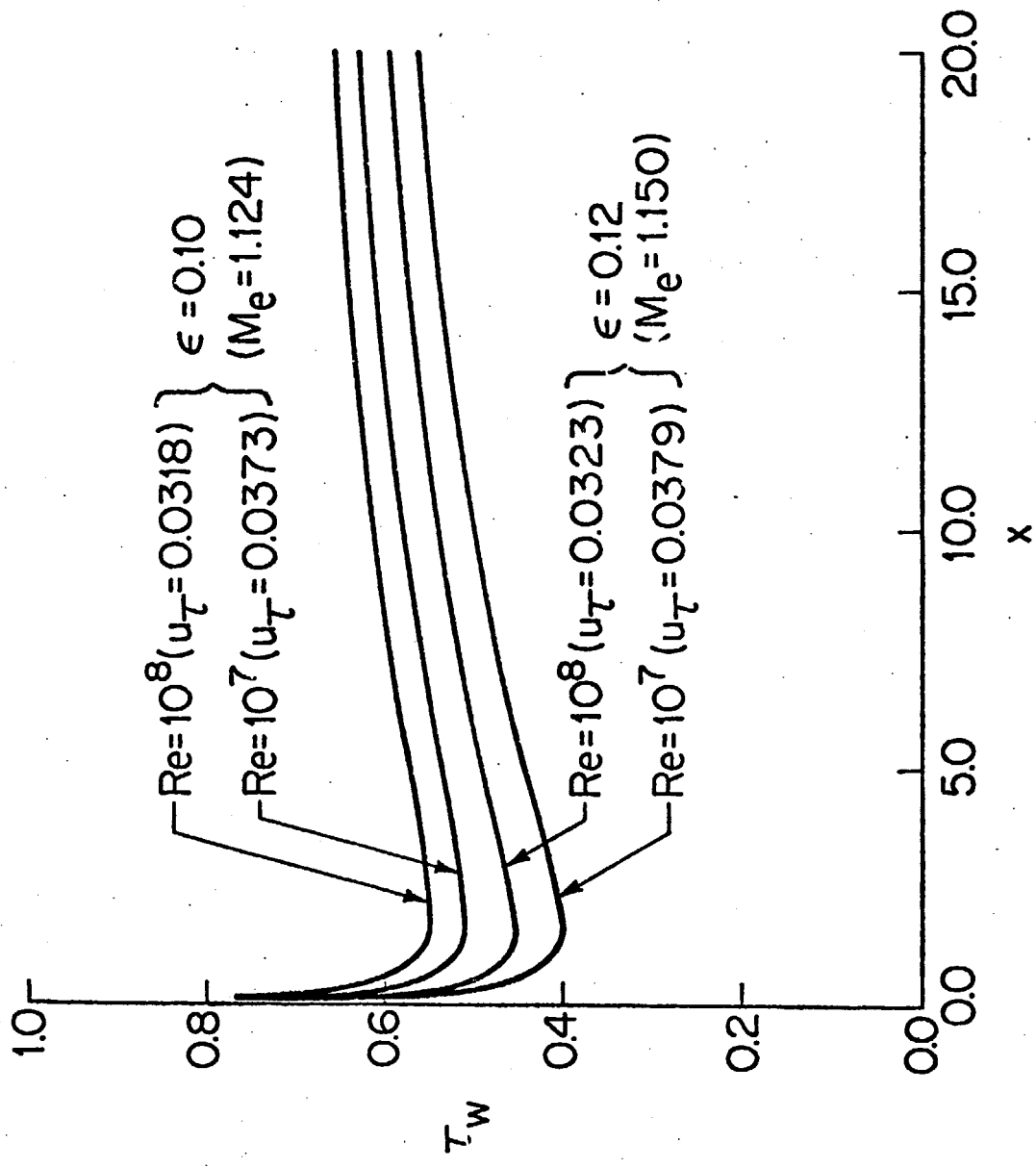


Figure 1. τ_w vs x for various values of Me and Re , for flow over a flat plate. (Eqn. (27a) with $\Pi = 0.5$, $K = 0$).

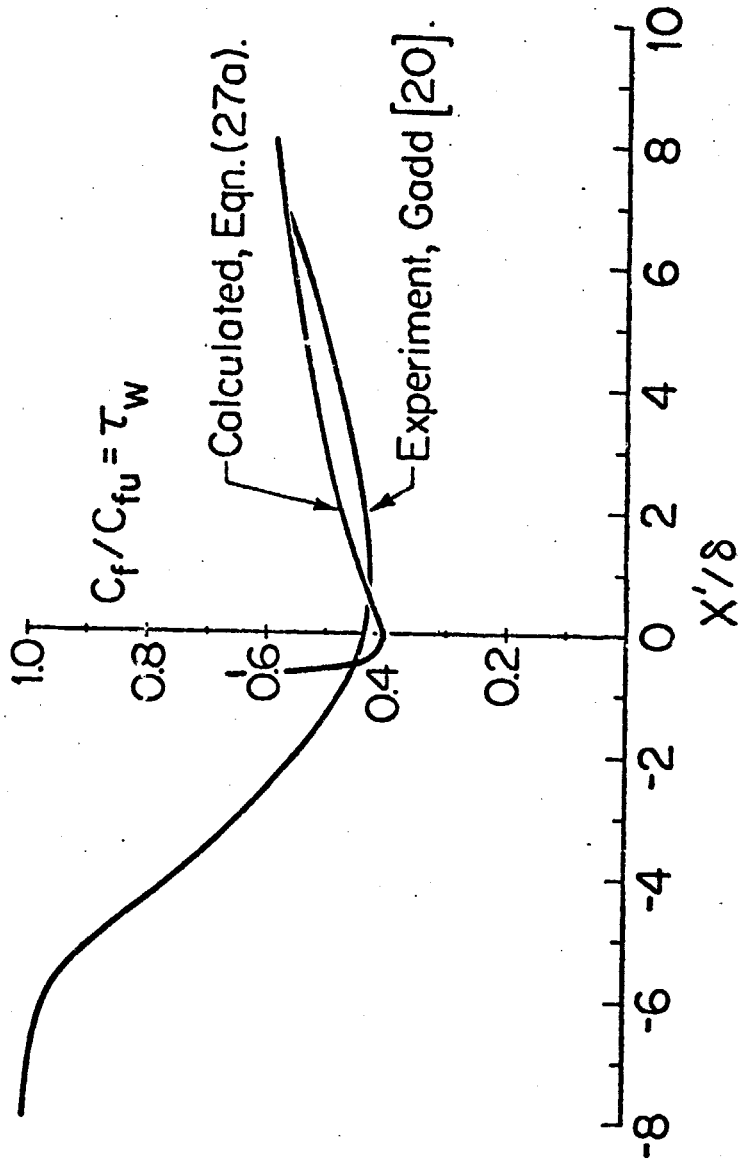


Figure 2. Comparison of calculated (eqn. (27a)) and experimental (ref. 20) values of c_f/c_{fu} vs X'/δ . Experimental conditions; $Me = 1.15$, $Re = 7 \times 10^6$, wall temperature = 15°C (59°F), $\overline{P}_{te} = 137.9 \text{ kPa}$ gauge (20 psig), $\overline{\delta} = 0.305 \text{ cm}$ (0.12 in.). Corresponding calculated parameters; $\epsilon = 0.120$, $u_\tau = 0.03968$, $\delta = 0.01634$, $\Pi = 0.312$, $K = 0$. $X'/\delta = 0$ at $P_w/P_{te} = 0.528$ from eqn. (7a).

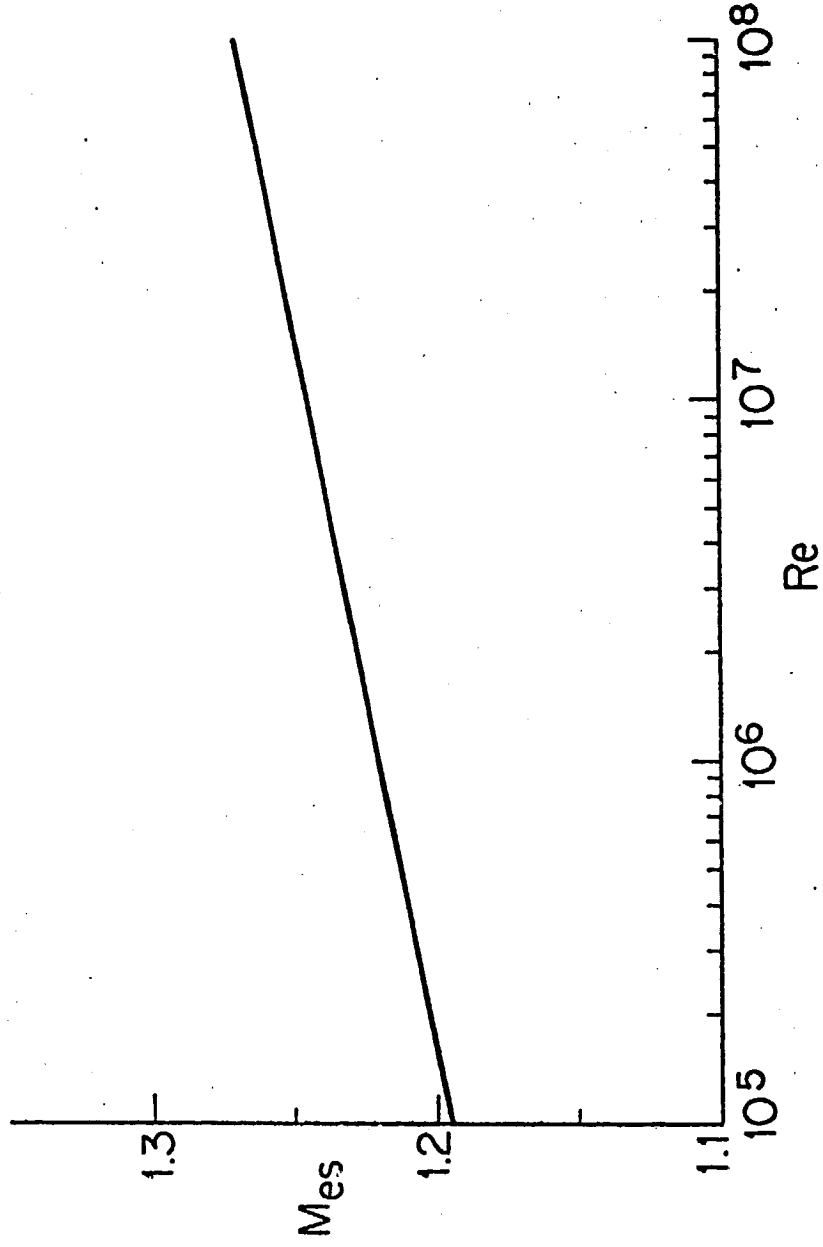


Figure 3. M_{es} (Mach number at incipient separation) vs Re for flow over a flat plate, calculated using eq. (27a) with $(\tau_w)_{min} = 0$, $\Pi = 0.5$; $K = 0$.